Journal of Physics: Conference Series

Cross-code verification of non-neutral ABL and single wind turbine wake modelling in LES

To cite this article: E L Hodgson *et al* 2023 *J. Phys.: Conf. Ser.* **2505** 012009

Journal of Physics: Conference Series **2505** (2023) 012009 doi:10.1088/1742-6596/2505/1/012009

Cross-code verification of non-neutral ABL and single wind turbine wake modelling in LES

E L Hodgson[1], M Souaiby[2], N Troldborg[3], F Porté-Agel[2] and S J Andersen[1]

[1] Technical University of Denmark, Department of Wind and Energy Systems, Anker Engelunds Vej 1, 2800 Kgs Lyngby, Denmark,

[2] Wind Engineering and Renewable Energy Laboratory (WIRE), École Polytechnique Fédérale de Lausanne (EPFL), 1015 Lausanne, Switzerland

[3] Technical University of Denmark, Department of Wind and Energy Systems, Frederiksborgvej 399, 4000 Roskilde, Denmark

E-mail: `emlh@dtu.dk`

Abstract. Large Eddy Simulations (LES) of atmospheric boundary layer (ABL) flow with the actuator disc (AD) for turbine modelling is a widely used method of simulating wind farm flows. Hence, it is important to understand the requirements for achieving a good comparison between ABL flow and turbine wakes between different research group setups, despite unavoidable differences which include LES numerical framework, sub-grid scale (SGS) model, and turbine modelling, and at grid resolutions achievable in large wind farm simulations. In this work, conventionally neutral (CNBL), stable (SBL) and convective (CBL) boundary layers, and single turbine wakes under these different conditions, are compared between the EPFL pseudo-spectral code WIRE LES and the DTU finite-volume code EllipSys3D. ABL profiles largely agree well with hub height velocity magnitudes agreeing to 0.7%, 3.8% and 0.5% for the CNBL, SBL and CBL respectively. The scale-dependent SGS model of WIRE LES results in reduced grid dependency, while EllipSys3D required higher grid resolution in the SBL. Wake flows show improved wake recovery and greater added turbulence intensity with increasing grid resolution, and good agreement is achieved with a radius R to cell size ratio of $R/(dxdydz)^{1/3} \geq 6.5$. Trends in wake flow with different stability conditions, such as the influence of inflow turbulence intensity or shear, are well replicated between codes. Likewise, wake deficit and added TI profiles, and distributions of turbine power and thrust also agree well. Mean power output predictions match to 4.3%, 7.2% and 3.8% in the CNBL, SBL and CBL respectively between the two codes. Overall, these results demonstrate that good agreement is possible with aligned turbine data and sufficient grid resolution.

1. Introduction

Large Eddy Simulation (LES) is an important tool for studying atmospheric boundary layer (ABL) flows and has been widely used to investigate various atmospheric conditions [1, 2, 3]. LES combined with the actuator disc (AD) [4] or actuator line (AL) [5] method for turbine modelling is a commonly used high-fidelity tool for simulating wind turbines and wind farms operating within the ABL. However, there are significant differences between the specific details of the numerical frameworks used by different research groups. Within ABL modelling, stable stratification is one of the most challenging conditions to simulate [3], but across all neutral and non-neutral conditions numerical dependencies can be seen, related to *e.g.* the LES code type, SGS model, and typical grid resolution [6, 7]. These choices can affect the generated wind velocity, turbulence, shear and veer. The modelling of wind turbines and wakes within the ABL is not only impacted by these factors [8], but also the differences in turbine modelling, such as the actuator model implementation, presence of aeroelastic coupling, and turbine controller [9, 10, 11]. This combination constitutes a large number of potential sources of uncertainty when conducting LES of wind turbines in the ABL.

In a comparison of four LES codes using laminar inflow and high resolution actuator line simulations, the numerical discretisation and Smagorinsky coefficient impacted the wake development by influencing the position at which the wake transitions to fully turbulent [12]. When even a small amount of inflow turbulence was introduced, it was the velocity fluctuations that dictated the wake breakdown location and hence good agreement was possible between setups. However, when moving from uniform laminar or non-sheared turbulent inflow to atmospheric boundary layer flows, variability in the inflow characteristics can provide significant challenges when comparing wake flows [13]. Under neutral conditions where numerical ABL flows were well-matched with measurements, wake predictions improved with model fidelity; whereas for a stable boundary layer case, single turbine wakes in the LES codes did not perform well due to different veer predictions from the precursor simulations. Likewise, when benchmarking LES simulations of very large wind farms [14], global trends (effect of turbulence intensity, 'infinite wind farm' velocity state, *etc*) compared well, but there was substantial variability in power and velocity averages both between codes and between the 10 minute averages within simulations.

Therefore, there is a need to investigate the requirements for achieving a high degree of similarity between wake flows predicted by different LES codes, when using ABL inflows, turbine modelling differs, and when conducted with grid resolutions which are achievable in large wind farm simulations. This is important not only for cross-code verification of ABL and turbine modelling, but also for informing future validation studies of both single wakes and wind farm flows. This study compares both ABL flow and turbine wakes in a range of atmospheric conditions between two well-validated and established LES codes, the DTU finite-volume code EllipSys3D and the EPFL pseudo-spectral code WIRE LES. First, inflow ABL simulations of conventionally neutral, stable and convective conditions are compared, considering the effect of grid resolution, domain size, numerical framework and SGS model. After the inflow conditions are aligned, the wake behind a single turbine is studied and the effect of turbine modelling parameters, turbine controller and grid resolution investigated.

2. Numerical Methods

2.1. EllipSys3D: DTU Flow Solver

EllipSys3D is a general purpose multi-block Navier-Stokes solver developed at DTU [15, 16, 17]. The incompressible governing equations (including the potential temperature transport equation to account for temperature effects) are expressed in general curvilinear coordinates and solved with a finite volume method in a collocated grid arrangement. Time advancement is performed using a second-order accurate three-level implicit method which has sub-iterations within each time step. To solve the pressure correction equation, a SIMPLEC-like algorithm is used [18, 19] with Rhie/Chow interpolation to prevent odd/even pressure decoupling. Convective terms are discretised with a fourth-order central differencing scheme which includes a fourth-order dissipation term to reduce numerical instabilities [20]. Turbulence modelling is achieved using Large Eddy Simulations (LES) with the Deardorff sub-grid scale (SGS) model [1]. In non-neutral cases, Monin-Obukhov similarity theory is applied at the lowest grid cell to calculate the instantaneous surface shear stress [21].

Wind turbines are modelled using the actuator disc (AD) method [4], which is fully coupled to the Flex5 aeroelastic solver [22]. EllipSys3D extracts the velocity components at the three rotating blade positions and passes them to Flex5, which calculates the blade loads and deflections using tabulated aerofoil data. These are used in EllipSys3D to set the position and magnitude of the actuator disc forces, which are applied to the computational grid in three overlapping 240° sections, in which the forcing decreases from a maximum at the blade location to zero at the neighbouring blades. This allows non-uniform loading to be represented. Flex5 includes a turbine controller, which changes the rotational speed and pitch in response to the calculated loading. Here, the turbine is modelled as stiff.

2.2. WIRE LES: EPFL Flow Solver

The WIRE LES code solves the spatially filtered incompressible Navier-Stokes equations [23, 24, 25]. Additionally, to account for the thermal effects, the filtered transport equation for potential temperature is solved. The turbulent subgrid-scale (SGS) momentum flux is modelled using a Lagrangian scale-dependent dynamic model [26]. For time advancement a second-order Adams-Bashforth explicit scheme is executed and for spatial discretization, a hybrid pseudo-spectral finite-difference scheme is applied. The spatial derivatives are evaluated using a pseudo-spectral method streamwise and spanwise resulting in a periodic boundary condition laterally and a second-order finite-difference approximation in the vertical direction. Full dealiasing of the nonlinear terms is accomplished by explicit filtering. At the bottom surface, the instantaneous surface shear stress is calculated as a function of the velocity field at the lowest vertical grid point by applying the Monin-Obukhov similarity theory [21].

The turbine-induced forces are modelled by the blade element actuator disc model (ADM-BE) for the wind farm parametrisation. Its implementation consists of calculating the lift and drag forces as a function of the local simulated flow and the blade characteristics [25]. This model induces wake rotation and allows for non-uniform distribution of the turbine-induced forces [27]. The airfoil data was the same as used in Flex5, and the turbine characteristic curves for rotational speed and pitch were provided from Flex5, in order to match the turbine modelling as closely as possible. It is also important to note that the rotational speed of the turbine in the cases with control is obtained using the modified thrust coefficient C_T' approach based on the averaged disc velocity rather than the unperturbed incoming velocity [28].

3. Simulation Setup

3.1. ABL simulations

The computational domains for all ABL simulations have spanwise and streamwise dimensions of approximately $4 \times 4km$ (For EllipSys3D the dimensions were $4.16 \times 4.16km$, and for WIRE LES $4{\times}4km$). The height of the domain varied for the different simulations depending on the inversion height that needed to be captured; $0.75km$, $1.5km$ and $2km$ for the stable, conventionally neutral and convective cases respectively. Periodic boundary conditions are used in streamwise and spanwise directions to facilitate the ABL development. The WIRE LES code has a flux-free condition at the upper boundary and a Rayleigh damping layer of 15% of the domain height, following the GEWEX Atmospheric Boundary Layer Study (GABLS) case description [29, 30], to reduce the reflection of gravity waves from the top of the domain. The EllipSys3D simulations use a small amount of grid stretching in the vertical direction above the inversion height.

The simulations comprise of three different stability cases - representing conventionally neutral, stable and convective conditions - based on canonical benchmark studies [3, 31]. Each of these cases is adapted to prevalent offshore conditions in Denmark as summarised in Table 1, where U_G is the geostrophic wind velocity, z_0 is the surface roughness, θ_0 is the reference potential temperature, dT/dz denotes the initial temperature profile and t_{total} refers to the total simulated time. The lower boundary condition (BC) is also given. Geostrophic wind is used to drive the flow, and wind direction controllers are used to achieve 0° at hub height at the domain centre. The Coriolis parameter used in all cases was $f_c = 1.185 \times 10^{-4} s^{-1}$.

Case	U_G $[m/s]$	z_0 $[m]$	$\theta_0[K]$	Initial Temp $[dT/dz]$	Lower BC	$t_{total}[h]$
CNBL	9.5	0.001	277	$0.001z$	$-$	27
SBL	9.5	0.001	277	$z < 100m : 0$ $z > 100m : 0.01z$	Cooling rate $dT/dt = -0.25K/h$	10
CBL	9.5	0.001	277	$z < 937m : 0$ $937 - 1063m : 0.0635z$ $z > 1063m : 0.003z$	Surface heat flux $Q_0 = 0.24Km/s$	5

Table 1. ABL simulation cases.

Each case is run with two grid resolutions, where the naming convention is '-1' for the coarser grid and '-2' for the finer. In EllipSys3D the cell sizes are $dx = dy = 2dz = 20m$ (DTU-1) and $dx = dy = 2dz = 10m$ (DTU-2) respectively (for the SBL a $dx = dy = 2dz = 5m$ (DTU-3) is also used). In WIRE LES the cell sizes are $dx = dy = 15.625m$, $dz = 11.72m$ (EPFL-1) and $dx = dy = 7.8125m$, $dz = 5.86m$ (EPFL-2) respectively. For the CBL cases in WIRE LES, the vertical resolution is slightly different: $dz = 7.8125m$ (EPFL-1) and $dz = 3.9m$ (EPFL-2). This is due to the increased domain height and computational restrictions on possible values for the number of grid points in the vertical direction (n_z), related to the set number of grid points in spanwise and streamwise. The last two hours of each simulation are used as inflow to the turbine simulations.

3.2. Single Turbine Simulations

The turbine used in these simulations is the SWT-2.3-93, a 2.3MW turbine with rotor radius $R = 46.5m$ and hub height $h = 68.5m$. It is chosen as it is the turbine used in the Rødsand II windfarm in Denmark, which will be involved in further work. To generate the inflow for the successor domain containing the turbine, velocity fields are written out from the precursor over the final 2 hours of each simulation. In EllipSys3D the velocity fields are written out from a vertical plane, while in WIRE LES a thin volume is used. These are taken from the domain centre, where the wind direction controller ensures that the direction is $0°$ at hub height. In the successor simulation WIRE LES uses a buffer zone at the inlet due to the periodic boundary conditions [32]. The EllipSys3D grid resolution in the single turbine cases is not constrained by the precursor, as the inflow data can be interpolated on to any arbitrary mesh. In WIRE LES the grid discretisation of the precursor and successor must be identical.

The set of simulations consists of two studies: a fixed control grid resolution study with the CNBL inflow; and an atmospheric stability study with control on, a single grid resolution and different ABL inflows. An overview of the single turbine simulations is shown in Table 2, showing the inflow case, grid resolution and turbine control inputs.

Case	Inflow	dx, dy $[m]$	dz $[m]$	$R/(dxdydz)^{1/3}$ [-]	Ω $[rad/s]$
EPFL$-1f$	CNBL	15.625	11.72	3.28	1.43
EPFL$-2f$	CNBL	7.8125	5.86	6.55	1.45
DTU$-0f$	CNBL	23.25	23.25	2.0	1.40
DTU$-1f$	CNBL	11.625	11.65	4.0	1.40
DTU$-2f$	CNBL	5.8125	5.8125	8.0	1.40
DTU$-3f$	CNBL	2.90625	2.90625	16.0	1.40
EPFL$-2c$	CNBL,SBL,CBL	7.8125	5.86, 3.9(CBL)	6.55, 7.50(CBL)	Control
DTU$-2c$	CNBL,SBL,CBL	5.8125	5.8125	8.0	Control

Table 2. Single turbine simulation cases.

In the grid study, rotational speeds for the EPFL cases are chosen in order to match the thrust coefficient (C_T) of the DTU simulations, to isolate the impact of grid resolution on the wakes. The naming convention of the simulations is based on the grid resolution and whether there is fixed ('f') or controller-based ('c') rotational speed and pitch. An increasing number ('-0' to '-3' for the DTU cases, '-1' and '-2' for EPFL) represents an increasing grid refinement. The inflow DTU-2 is used for all DTU single turbine simulations except the SBL, where DTU-3 is used. The inflow EPFL-2 is used in EPFL$-2f$ and EPFL$-2c$ simulations. Due to the required match between precursor and successor domains in WIRE LES, the inflow EPFL-1 is used for the EPFL$-1f$ single turbine simulation.

4. Results

4.1. Atmospheric Boundary Layer Simulations

The conventionally neutral, stable and convective cases were run for a total of 27, 10 and 5 hours respectively, with horizontally averaged profiles taken from the final 2 hours. In all simulations, a quasi-steady state was obtained in the velocity and turbulence intensity profiles before the start of the averaging period. Mean profiles of velocity magnitude (U_{mag}), resolved turbulent kinetic energy (TKE) and temperature (T) are shown in Figure 1, while quantities at hub height for the finest grid simulations are detailed in Table 3.

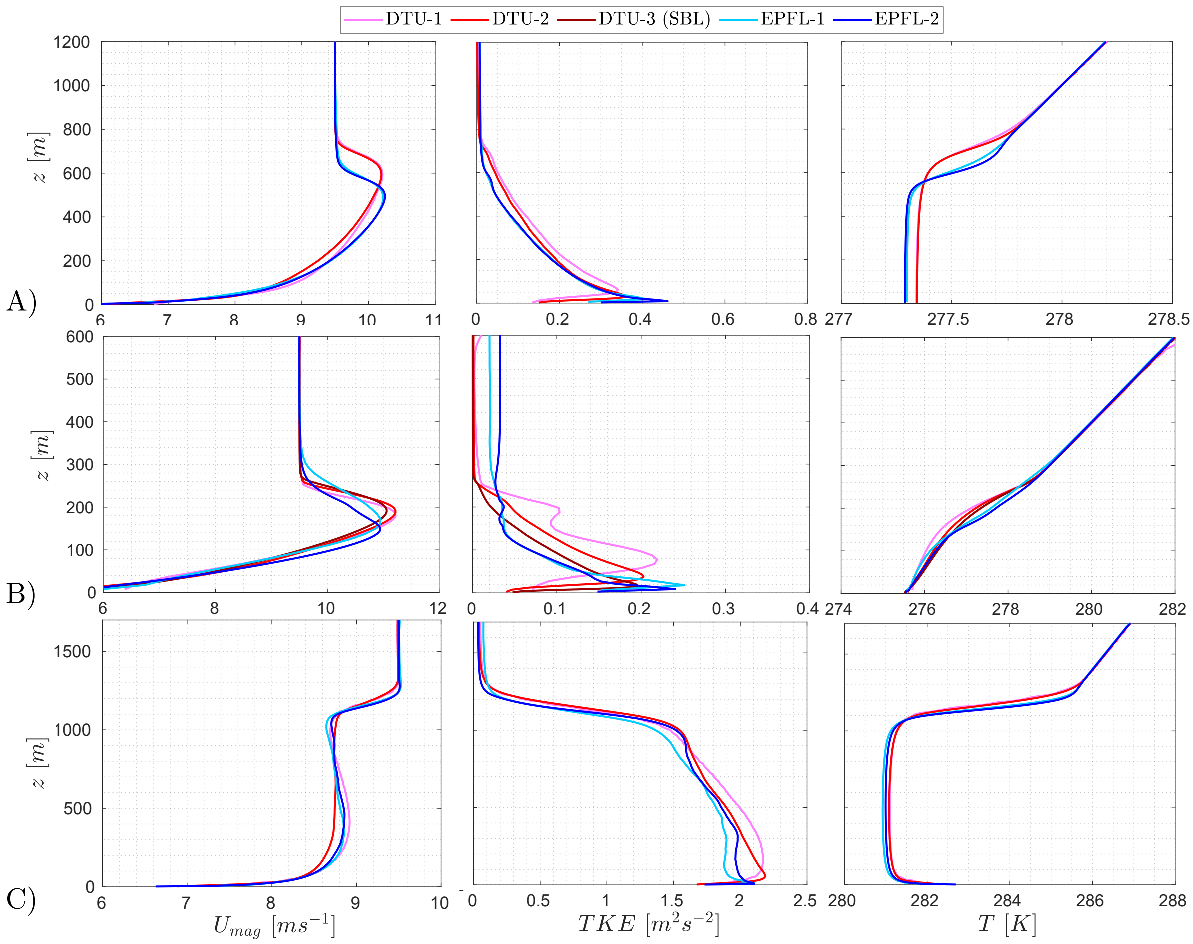

Figure 1. Horizontally averaged profiles of velocity magnitude (U_{mag}), resolved turbulent kinetic energy (TKE) and temperature (T): A) CNBL; B) SBL; C) CBL.

Case	CNBL			SBL			CBL		
	EPFL-2	DTU-2	$\Delta[\%]$	EPFL-2	DTU-3	$\Delta[\%]$	EPFL-2	DTU-2	$\Delta[\%]$
$U_{hub}\ [ms^{-1}]$	8.457	8.401	0.7	8.958	8.630	3.8	8.415	8.372	0.5
$TI_{Uhub}\ [-]$	0.0520	0.0529	1.7	0.0296	0.0332	10.8	0.1369	0.1458	6.5
$U_*\ [ms^{-1}]$	0.294	0.305	3.7	0.246	0.260	5.7	0.356	0.372	4.5
$L\ [m]$	-	-	-	110	123	10.6	-15.0	-15.5	2.9

Table 3. Velocity magnitude at hub height (U_{hub}), total TI at hub height (TI_{Uhub}), friction velocity (U_*) and Obukhov length (L) for the finest grid ABL simulations.

In both Table 3 and the mean profiles in Figure 1, there is largely good agreement in the ABL flows despite the differences between LES codes; particularly in the mean velocity magnitude at hub height, which differs by 0.7%, 3.8% and 0.5% for the CNBL, SBL and CBL cases respectively for the finest grid simulations.

For the CNBL, the TI predictions also match well at hub height, with only a 1.7% difference between the two codes. The largest discrepancy between EPFL and DTU CNBL precursors is the predicted boundary layer height, which is $130m$ higher for the DTU simulations, although it appears to have little impact on the good agreement in the surface layer. The change in the hub height velocity between coarse (-1) and fine (-2) simulations is 1.6% for both codes; for the TI the change is 0.8% for WIRE LES, and 4.3% in EllipSys3D. The larger grid dependency of the EllipSys3D simulations is visible in the TKE profile as a downward shift in the peak near the ground; this is also present in the WIRE LES simulations but to a lesser degree, and further below hub height. The differences here may be due to the SGS model. The Deardorff SGS model used in EllipSys3D calculates eddy viscosity using a constant model coefficient $C_s = 0.1$ and a mixing length which differs from the grid size under stable conditions; while the Lagrangian scale-dependent dynamic model used in WIRE LES calculates a local optimum model coefficient value based on two test-filtering operations. The scale dependency has been shown to improve performance and reduce grid dependency, particularly in the near ground region, by capturing the reduction in optimum model coefficient independent of grid size [24]. An increased grid resolution improves the EllipSys3D simulations due to explicitly resolving a larger proportion of the total TKE, despite the ratio of resolved to total TKE being greater than 95% (over the recommended 80% [33] or 90% [34]) except in the lowest 50m of the domain, due to the Deardorff mixing length parameterisation not being altered by the presence of a surface (see [35]).

SBLs are often the most difficult to simulate and compare ([3, 13]), so it is unsurprising that it is this case in which differences are most pronounced between both codes and grid resolutions. In EllipSys3D, the increased grid resolution again lowers the height of peak TKE, however it is far more pronounced than for the CNBL. The inversion height of the SBL is significantly lower than that of the other stability cases, and therefore the ratio of inversion height to grid cell size is far worse. This is likely to contribute to the poorer grid convergence as the boundary layer is effectively resolved by fewer cells. Sullivan and Patton [6] recommended a ratio of inversion height z_i to grid cell size (expressed in terms of filter length Δ_f) of $z_i/\Delta_f > 60$ when studying CBLs. This condition is met in both DTU-1 and DTU-2 for the CBL, DTU-2 for the CNBL, but only the finest (DTU-3) for the SBL. This may explain the poorer grid convergence for the SBL, particularly in the EllipSys3D simulations using the Deardorff SGS model.

The CBL cases again agree well in the surface layer, with velocity magnitude and TI predictions within 0.5% and 6.5% respectively between the two codes. The inversion height predictions also match closely, which may be due to the shorter simulation time and the strong prescribed inversion in the initial conditions. However, the shape of the velocity profile has some grid dependency; similar to the CNBL, a coarser grid causes an overestimation of velocity magnitude in the region above the surface layer.

To compare the dynamics of the ABL simulations, spectra of the streamwise component of velocity are shown in Figure 2. The spectra are calculated at hub height, horizontally averaging along a 500m spanwise line at the domain centre. Also included in the CNBL plot is one case in EllipSys3D on a 16×16 km domain to show the impact of domain size.

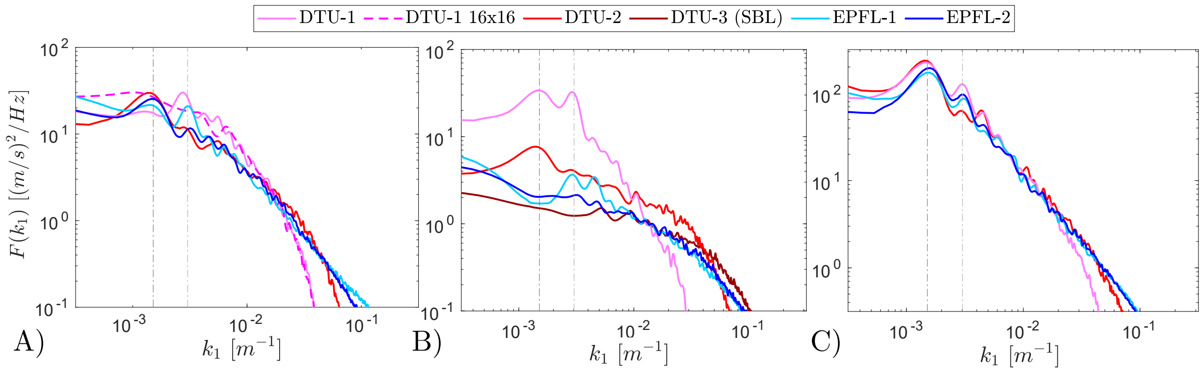

Figure 2. Spectral energy density against wavenumber for streamwise velocity component for: A) CNBL; B) SBL; C) CBL. Domain size in grey and half of the domain size in light grey.

Reflecting the comparisons of the mean profiles, in the CNBL results the hub height velocity spectra compare well except the coarse DTU−1 simulation, which shows a higher energy content at lower wavenumbers and earlier drop-off in the spectra at high wavenumbers. For the SBL, it is unsurprising given the differences in TKE profiles that there are substantial differences in the spectra between the DTU simulations, while the EPFL results still agree well between the two grid levels. However, the comparison between the finest grid DTU simulation (DTU−3) and the EPFL cases is significantly improved. In the CBL simulations, all cases agree well: for EPFL−1 and EPFL−2 this is expected due to the higher grid resolution in the vertical dimension, but also DTU−1 and DTU−2 show a less pronounced difference at lower wavenumbers. Like with the mean profiles, differences in grid dependency can be explained by the SGS model and the ratio of inversion height to grid cell size. The drop off in spectra in the DTU simulations is similar to that noted for Smagorinsky-type models [24] and signals excessive dissipation at low heights, while the Lagrangian dynamic scale-dependent model leads to better estimation of the model coefficient and hence more consistent spectra.

The 4×4 km domain simulations of CNBL or CBL conditions show spectral peaks related to the domain size (marked in grey and light grey lines). The finest grid SBL cases (DTU−3 and EPFL−2) do not show these peaks. Stable stratification results in lower integral length scales than neutral or convective conditions [36], as they contain buoyancy effects that suppress large turbulent scales. This means the domain size is likely to be less apparent in the spectra, and hence that the fine grid SBL simulations capture this suppression of turbulence better than the coarse grids. For the CNBL and CBL cases, the domain size effect is removed when a much larger domain (16×16 km) is used in the DTU−2 CNBL; demonstrating the need to use large domain sizes or other techniques to avoid spurious large scale effects [37].

4.2. Single Turbine Wakes

To investigate the impact of turbine modelling and grid resolution on the wakes without the influence of turbine control, the first comparison using the CNBL inflow is conducted with fixed rotational speed (listed in Table 2) to ensure that the thrust coefficient (C_T) matches between the EllipSys3D and WIRE LES setups. The inflow for the DTU simulations is case DTU−2 (the finer grid); the EPFL simulations require that the precursor and turbine grid resolutions match, so both inflows are used. The final 2 hours of the precursor simulations are used as inflow and statistics are taken from the final hour. The grid convergence of mean C_T is shown in Figure 3, and profiles of normalised mean velocity deficit and added TI are shown in Figure 4.

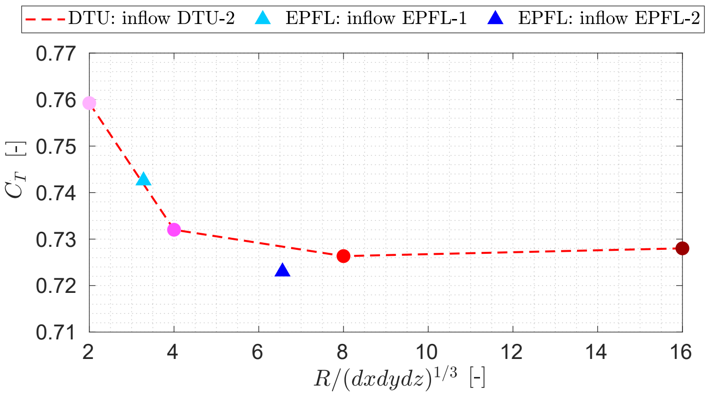

Figure 3. Thrust coefficient (C_T) against grid resolution for CNBL inflow.

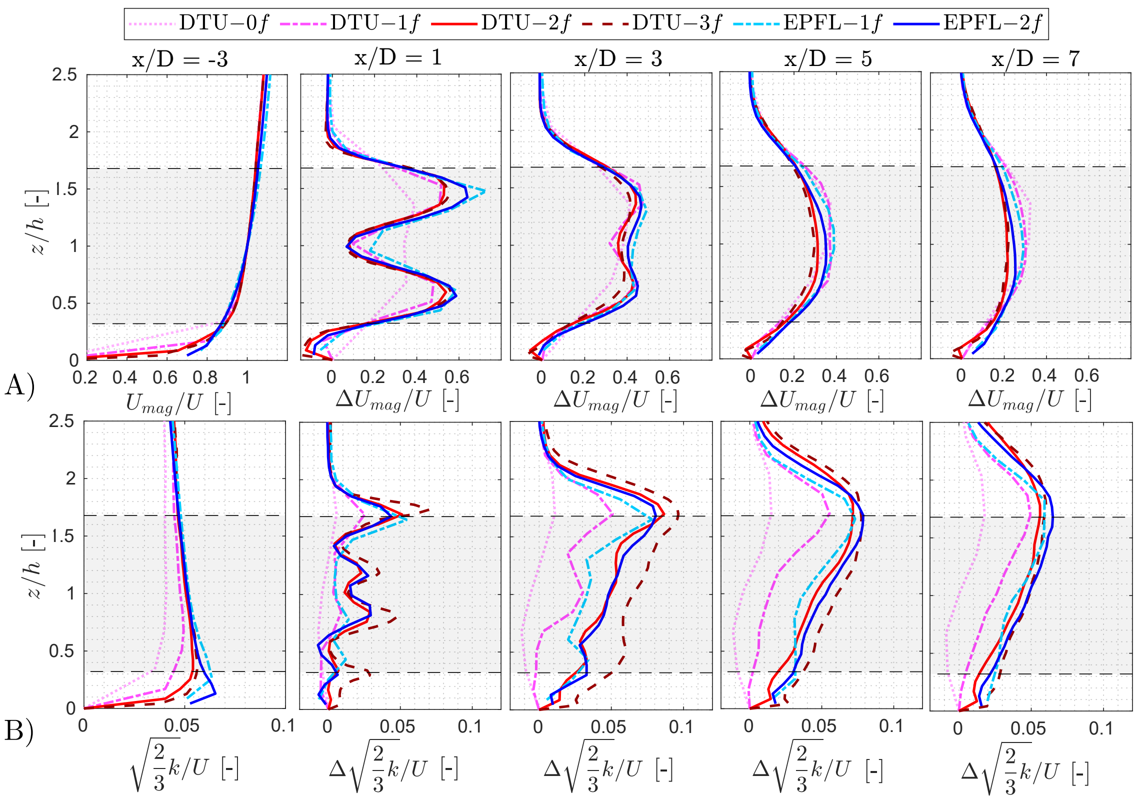

Figure 4. Wake profiles for CNBL inflow: A) velocity deficit normalised by freestream hub height velocity; B) total added TI based on hub height velocity. Rotor extent in grey.

Figure 3 shows that the mean C_T values agree to within 2.7% when excluding DTU−0f ($R/(dxdydz)^{1/3} = 2$), which from both the C_T and wake profiles is clearly too coarse. Therefore, differences in normalised wake flow can be primarily attributed to the grid resolution. Other grid studies in EllipSys3D using laminar [11] or uniform turbulent inflow [38] have shown convergence of C_T to within 1% for a stiff AD at $R/(dxdydz)^{1/3} \geq 8$, or for a flexible AL at $R/(dxdydz)^{1/3} \geq 16$ (both using uniform grids). The grid study results here, for a CNBL inflow, give a difference in mean C_T between $R/(dxdydz)^{1/3} = 8$ and 16 of only 0.2%, and so is consistent with previous findings in EllipSys3D.

Considering the velocity deficit and added TI plots, it is clear that the same trends exist in both the EllipSys3D and WIRE LES results. Increasing the grid resolution results in an increased TI production and a smaller velocity deficit in the far wake. This improved wake recovery is associated with more finely resolving the shear layer shed from the disc and the entrainment into the wake region. It is notable that in both the velocity deficit and TI production, simulation EPFL$-1f$ largely lies between DTU$-1f$ and DTU$-2f$, suggesting that the more advanced SGS model may somewhat improve the grid dependency of the turbine wakes as well as the precursor simulations. The three finer grid simulations show very good agreement overall, particularly in the far wake. The normalised mean hub height velocity deficits are 0.219, 0.213 and 0.248 for DTU$-3f$, DTU$-2f$ and EPFL$-2f$ respectively at $x/D = 7$; so the velocity magnitude predictions differ there by only 3.9%. Based on the convergence of these three simulations, a grid resolution requirement of $R/(dxdydz)^{1/3} \geq 6.5$ is used for the non-neutral turbine simulations. This recommendation of $R/(dxdydz)^{1/3} \geq 6.5$ for an AD wake is finer than some prior recommendations of $R/(dxdydz)^{1/3} \geq 4$ [25].

When conducting LES of wind farms, turbine rotational speed and pitch are not fixed, but continuously altered by a controller. In WIRE LES, this is done using an inflow velocity found using the C'_T method [28] and characteristic steady-state curves (here provided by Flex5). In the DTU setup the Flex5 controller is used, which responds to the calculated loading. Having established that good agreement can be achieved in wake flow given that the C_T values match, when using a grid resolution of $R/(dxdydz)^{1/3} = 6.5$ or greater, the turbine operation and wakes are compared with controllers active for the three ABL inflows using EPFL$-2c$ ($R/(dxdydz)^{1/3} = 6.55$, or 7.5 for CBL) and DTU$-2c$ ($R/(dxdydz)^{1/3} = 8$). Mean velocity deficit and added TI profiles are shown in Figure 5, with statistics again taken over the final 1 hour of the 2 hour simulation.

The inflow profiles of normalised velocity and TI agree well between the codes, with the DTU simulations showing a slightly increased shear over the rotor area compared to EPFL across all three cases, reflecting the results from the precursor comparisons. For the wake flow, trends between the different ABL inflows are also predicted very similarly between WIRE LES and EllipSys3D. The most deterministic factor is the inflow TI; the CBL case has more than 2.5× greater TI than the CNBL or SBL case, so the wake recovers significantly faster, reaching a Gaussian wake profile between $x/D = 1$ and 3, while for both the CNBL and SBL this happens between $x/D = 3$ and 5. Another way the different ABL cases impact the wake development stems from the inflow shear; for both codes the SBL case shows very little expansion of the wake vertically upwards in comparison to the CNBL, and less TI increase above the rotor area.

Despite the overall good agreement, there are some differences in wake profiles attributable to the AD models. In Figures 4 and 5, there is a difference in velocity deficit between the upper and lower half of the near wake in the WIRE LES results, which is not present in EllipSys3D. In the DTU AD model, the coupling with Flex5 means the local velocity components are extracted at three rotating ‘blade’ locations and the calculated loading is distributed over three overlapping 240° sections (closer to an AL approach); whereas in the EPFL AD model the local velocities are extracted and forces calculated for each element of the actuator disc grid. This means that the difference between the mean thrust force at the top and bottom of the rotor is greater in the EPFL AD model when averaged over a rotation, and therefore the wake profile is less symmetric. This may contribute to the larger velocity deficit of the EPFL simulations in the far wake.

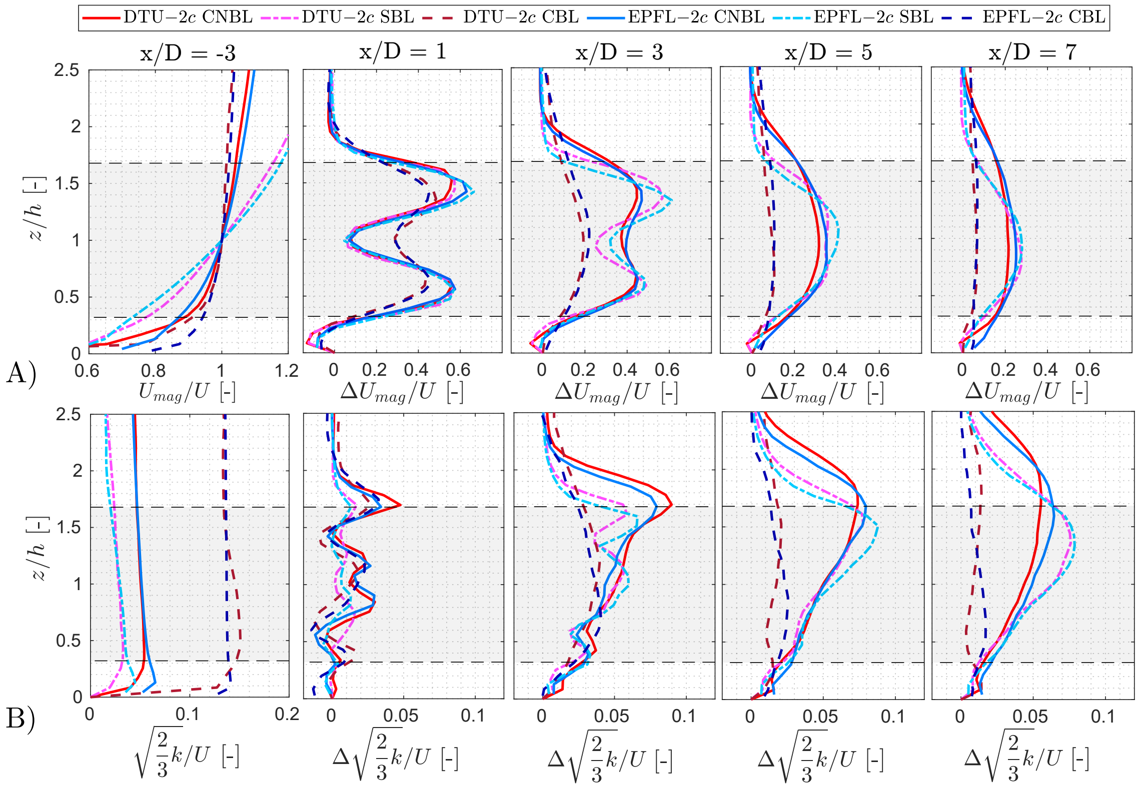

Figure 5. Wake profiles for different ABL inflows with turbine control on: A) velocity deficit normalised by freestream hub height velocity; B) total TI based on freestream hub height velocity. Rotor extent in grey.

In addition to studying the wake flows, it is important to compare the turbine performance predictions under the different ABL inflows. Violin plots of normalised power and thrust from both turbine models for each stability condition are shown in Figure 6, using 1s sampling over the final hour of each simulation.

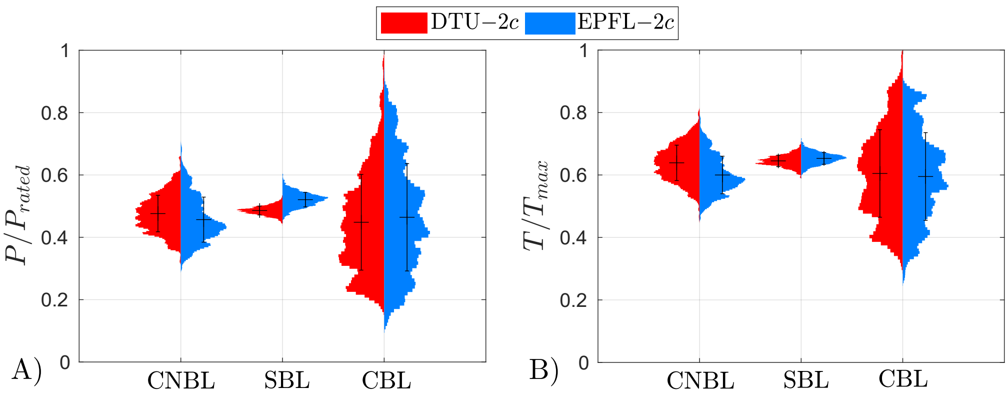

Figure 6. Turbine performance under different inflow stability conditions: A) Normalised power (P/P_{rated}); B) Normalised thrust (T/T_{max}). Mean and standard deviation in black.

Following from the good agreement in both atmospheric inflow profiles and wake flows, the distribution plots again show close agreement between turbine performance predictions, in both the distribution means, shape and spread. The mean power output values, when including the mechanical losses from Flex5 in both EPFL and DTU results, have percentage differences of 4.3%, 7.2% and 3.8% for the CNBL, SBL and CBL cases respectively, between the EPFL and DTU simulations. The mean thrust values differ by 6.4%, 1.4% and 1.5% respectively. For the CNBL case, it should be noted that the percentage difference in mean thrust is larger than in the grid study (6.4% compared to $\leq 0.2\%$), in which the rotational speed was set in order to match the C_T. Despite this, the wake profiles in Figure 5 only vary slightly more than in Figure 4. Even though the inflow hub height velocities differ by only 0.7% (as listed in Table 3), a slightly higher rotational speed was required in the EPFL$-2f$ case to match the DTU$-2f$ C_T in the grid study, which could be attributable to the different AD implementations. The offset towards a lower thrust prediction in EPFL$-2c$ in a case where the inflows are very closely aligned is likely to explain why the SBL and CBL appear to agree better in thrust than the CNBL, as in both of these cases the EPFL-2 inflow velocity was higher than DTU-2.

The similarity in the spread and shape of the distributions between DTU and EPFL simulations reflects the agreement in both inflow turbulence intensity and predominant turbulent length scales. It also suggests that for a single turbine case, the different control methods do not substantially influence the variability of the turbine outputs. Overall, agreement in mean power to $\leq 7.2\%$ and mean thrust to $\leq 6.4\%$ between two different research group frameworks is significantly closer than in large benchmark studies [13], particularly when comparing across a range of non-neutral ABL inflows. The percentage differences are similar to that achieved using EllipSys3D and identical sheared inflow when comparing AL to a fully resolved rotor [38].

5. Conclusions

LES of non-neutral ABL precursors and single turbines have been compared for conventionally neutral, stable and convective conditions, between the DTU flow solver EllipSys3D and the EPFL code WIRE LES. In the precursor simulations, at hub height for a 2.3 MW turbine, the mean velocity magnitudes differed by 0.7%, 3.8% and 0.5% for the CNBL, SBL and CBL respectively. The Lagrangian scale-dependent dynamic SGS model used in WIRE LES results in reduced grid dependency in both mean profiles (particularly TKE) and velocity spectra. The lower inversion height in the SBL case meant that a finer grid resolution was required in EllipSys3D than for the other stability cases. Across all precursors, the discrepancies grew outside of the surface layer, and so a significantly larger turbine would experience larger inflow differences.

In the single turbine cases, both grid resolution and the impact of inflow stability were investigated. In the grid study, when the C_T was matched the wake predictions showed the same trends: improving wake recovery and greater TKE production with increasing grid resolution. Good agreement was achieved with grid resolutions of $R/(dxdydz)^{1/3} = 6.5$ or finer; TKE production and velocity deficit profiles matched well throughout the wake, and at $x/D = 7$ downstream the hub height velocity magnitudes agreed to within 4%.

Using $R/(dxdydz)^{1/3} = 6.5$ in WIRE LES and $R/(dxdydz)^{1/3} = 8$ in EllipSys3D, wakes and integrated quantities were then compared with turbine control on using all three ABL cases. Trends under different stability conditions such as the influence of inflow TI and shear were well replicated between codes. Some differences can be attributed to the AD models; the DTU AD has loading based on three rotating blade locations and applied in overlapping 240° sections, while the EPFL AD uses a blade element grid covering the entire rotor area. This leads to a more symmetric normalised wake deficit profile in the near wake for the DTU AD model. However, good agreement was achieved in the far wake velocity deficits and the turbine power and thrust outputs, which gave very closely matching distributions in mean, shape and spread. Mean power outputs differed by 4.3%, 7.2% and 3.8% respectively for the CNBL, SBL and CBL cases respectively, and mean thrust by 6.4%, 1.4% and 1.5%. These results show that with sufficient grid resolution and alignment of turbine parameters, ABL inflows and single turbine wakes can agree well between codes despite differences in LES and turbine modelling setups.

Acknowledgements
The PhDs of Emily Louise Hodgson and Marwa Souaiby are funded by the European Union Horizon 2020 research and innovation program, Train2Wind project, grant agreement no. 861291. Proprietary data for the Siemens-Gamesa SWT-2.3-93 turbine is used. All DTU simulations were performed on the DTU cluster Sophia [39].

References

[1] Deardorff J W 1980 *Boundary-Layer Meteorology* **18** 495–527
[2] Moeng C H 1984 *Journal of Atmospheric Sciences* **41** 2052 – 2062
[3] Beare R J et al 2006 *Boundary-Layer Meteorology* **118** 247–272 ISSN 00068314
[4] Mikkelsen R 2004 *Actuator Disc Methods Applied to Wind Turbines* Ph.D. thesis
[5] Sørensen J N and Shen W Z 2002 *Journal of Fluids Engineering, Transactions of the ASME* **124**
[6] Sullivan P P and Patton E G 2011 *Journal of the Atmospheric Sciences* **68** 2395–2415 ISSN 00224928
[7] Brown A R, Cederwall R T, Chlond A, Duynkerke P G, Golaz J C, Khairoutdinov M, Lewellen D C, Lock A P, MacVean M K, Moeng C H, Neggers R A J, Siebesma A P and Stevens B 2002 *Quarterly Journal of the Royal Meteorological Society* **128** 1075–1093
[8] Abkar M and Porté-Agel F 2015 *Physics of Fluids* **27** ISSN 10897666
[9] Troldborg N, Zahle F, Réthoré P E and Sørensen N N 2015 *Wind Energy* **18** ISSN 10991824
[10] Stevens R J, Martínez-Tossas L A and Meneveau C 2018 *Renewable Energy* 470–478 ISSN 18790682
[11] Hodgson E L, Andersen S J, Troldborg N, Meyer Forsting A R, Mikkelsen R F and Sørensen J N 2021 *Journal of Physics: Conference Series* **1934**(1) ISSN 17426596
[12] Martínez-Tossas L A et al 2018 *Journal of Renewable and Sustainable Energy* **10** ISSN 19417012
[13] Doubrawa P et al 2020 *Wind Energy* **23** 2027–2055 ISSN 10991824
[14] Andersen S J, Breton S P, Witha B, Ivanell S and Nørkær Sørensen J 2020 *Wind Energy Science* **5** 1689–1703
[15] Sørensen N N 1995 *General Purpose Flow Solver Applied to Flow over Hills* Ph.D. thesis DTU
[16] Michelsen J A 1992 Basis3D – a Platform for Development of Multiblock PDE Solvers Tech. rep. DTU
[17] Michelsen J A 1994 Block structured multigrid solution of 2D and 3D elliptic PDE's Tech. Rep. AFM DTU
[18] Shen W Z, Michelsen J A, Sørensen N N and Sørensen J N 2003 *Numerical Heat Transfer, Part B: Fundamentals* **43** 221–239
[19] Kobayashi M H and Pereira J C F 1991 *Numerical Heat Transfer, Part B: Fundamentals* **19** 243–262
[20] Wit L and van Rhee C 2013 *Flow, Turbulence and Combustion* **92**
[21] Monin A and Obukhov A M 1954 *Trans. Geophys. Inst. Akad. Nauk.* **24** 163–187
[22] Øye S 1996 Flex4 simulation of wind turbine dynamics Tech. rep. DTU Lyngby, Denmark
[23] Albertson J D and Parlange M B 1999 *Water Resources Research* **35** 2121–2132
[24] Porté-Agel F, Meneveau C and Parlange M B 2000 *Journal of Fluid Mechanics* **415** 261–284 ISSN 0022-1120
[25] Wu Y T and Porté-Agel F 2011 *Boundary-Layer Meteorology* **138**(3) ISSN 00068314
[26] Stoll R and Porté-Agel F 2006 *Water Resources Research* **42**
[27] Porté-Agel F, Wu Y T, Lu H and Conzemius R J 2011 *Journal of Wind Engineering and Industrial Aerodynamics* **99** 154–168
[28] Meyers J and Meneveau C 2010 *48th AIAA Aerospace Sciences Meeting Including the New Horizons Forum and Aerospace Exposition*
[29] Lu H and Porté-Agel F 2011 *Physics of Fluids* **23**
[30] Stoll R and Porté-Agel F 2009 *Journal of the Atmospheric Sciences* **66** 412–431
[31] Moeng C H and Sullivan P P 1994 *Journal of Atmospheric Sciences* **51** 999 – 1022
[32] Wu Y T and Porté-Agel F 2015 *Renewable Energy* **75** 945–955
[33] Pope S B 2004 *New journal of Physics* **6** 35
[34] Matheou G and Chung D 2014 *Journal of the Atmospheric Sciences* **71** 4439–4460
[35] Dai Y, Basu S, Maronga B and de Roode S R 2021 *Boundary-Layer Meteorology* **178** 63–89 ISSN 15731472
[36] Peña A 2019 *Journal of Renewable and Sustainable Energy* **11** ISSN 19417012
[37] Munters W, Meneveau C and Meyers J 2016 *Physics of Fluids* **28** ISSN 10897666
[38] Hodgson E L et al 2022 *Frontiers in Energy Research* **10** ISSN 2296-598X
[39] DTU Computing Center 2021 DTU Computing Center resources